

Buckling of Shells

An internship report submitted
in partial fulfillment for the award of the certification for

Summer Internship 2025

by

Divya Choudhary



**Department of Aerospace Engineering
Indian Institute of Space Science and Technology
Thiruvananthapuram, India**

July 2025

Certificate

This is to certify that the internship report titled *Buckling of Shells* submitted by **Divya Choudhary**, to the Indian Institute of Space Science and Technology, Thiruvananthapuram, in partial fulfillment for the award of the certification for the **Summer Internship 2025** is a bona fide record of the original work carried out by him/her under my supervision. The contents of this internship report, in full or in parts, have not been submitted to any other Institute or University for the award of any degree or diploma.

Dr S. Anup

Professor,
Department of Aerospace Engineering,
IIST, Thiruvananthapuram

Dr M. Deepu

Professor and Head,
Department of Aerospace Engineering,
IIST, Thiruvananthapuram

Place: Thiruvananthapuram

Date: July 2025

Declaration

I declare that this internship report titled *Buckling of Shells* submitted in partial fulfillment for the award of the degree of **Summer Internship 2025** is a record of the original work carried out by me under the supervision of **Dr S. Anup**, and has not formed the basis for the award of any degree, diploma, associateship, fellowship, or other titles in this or any other Institution or University of higher learning. In keeping with the ethical practice in reporting scientific information, due acknowledgments have been made wherever the findings of others have been cited.

Place: Thiruvananthapuram

Divya Choudhary

Date: July 2025

(IS00646)

Acknowledgements

I would like to express my sincere gratitude to Prof. S. Anup for his invaluable guidance, constant encouragement, and insightful feedback throughout the course of this project. His deep expertise and thoughtful mentorship have been instrumental in shaping the direction and quality of my work. I am truly thankful for the opportunity to learn under his supervision and for the support he has extended at every stage of this study.

Divya Choudhary

Abstract

This project explores the buckling behavior of dished shallow shells subjected to uniform external pressure, with particular emphasis on the influence of geometric imperfections. Such shells—commonly used in aerospace, marine, and structural applications are prone to sudden snap-through buckling, making reliable design essential.

A finite element framework was established in Abaqus, employing S4R shell elements to model the dished geometry and material properties representative of thin metallic shells. Both linear eigenvalue analysis and nonlinear Riks analysis were used to investigate ideal (perfect) shell responses, capturing critical buckling modes and postbuckling paths.

To account for manufacturing irregularities, two imperfection strategies were implemented: localized dimples introduced via static displacement fields, and spatially correlated random thickness variations generated through a spectral representation of a prescribed power spectral density function. These imperfections were superimposed on the nominal shell geometry to create a suite of imperfect models.

A probabilistic workflow was developed to integrate imperfection statistics into buckling analysis, enabling the extraction of knock-down factors from load-deflection curves. The methodology lays the groundwork for a reliability-based design approach, linking imperfection characteristics to buckling performance in dished shallow shells.

Contents

List of Figures	xi
List of Tables	xiii
Nomenclature	xv
1 Introduction	1
1.1 Dished Shallow Shells	1
1.2 Snap-Through Buckling	2
1.3 Random Geometric Imperfections	3
1.4 Objective	4
1.5 Approach	5
2 Effect of Linear and Non-Linear Analysis and Dimple Imperfections	6
2.1 Methodology	6
2.2 Model Description	7
2.3 Eigenvalue Analysis and Riks Analysis	8
2.4 Dimple Imperfections	9
3 Random Geometric Imperfections	11
3.1 Background	11
3.2 Methodology	11
4 Results and Discussion	13
4.1 Eigenvalue and Riks Analysis	13
4.2 Dimple Imperfections	14
4.3 Random Imperfections	14

5 Conclusion	20
6 References	22
Appendices	23
A Methodology for Generating Random Thickness Imperfections	23
A.1 Overview	23
A.2 Implementation Details	23
A.3 Code Availability	24

List of Figures

1.1	Schematic of a control component in which a dished shell is used as an actuator element (Thesis, Surya Mani Tripathi, 2022)	2
1.2	Snap-through or Limit Point buckling of a spherical cap under uniform external pressure (S.M. Tripathi, D. Swain, R. Muthukumar, and S. Anup, 2020)	3
2.1	A typical dished shell under uniform pressure adopted from Liu et. al. Dong and Shanlin (1997)	6
2.2	Boundary conditions: Pressure load and Fixed bottom edge	7
2.3	Quad mesh with element size of 0.25mm - Total of 62929 elements	8
2.4	Buckling mode shapes for shell of dimensions $a=30\text{mm}$, $b=15\text{mm}$, $H=3\text{mm}$, $t=0.3\text{mm}$	9
2.5	Boundary conditions used for static (left) and riks (right) analyses.	10
3.1	Sample Random field for thickness variation	12
4.1	Load Proportionality Factor versus Displacement, Elastic Material, $a=30\text{mm}$, $b=15\text{mm}$, $H=3\text{mm}$, $t=0.3\text{mm}$, Load Applied: 0.33380 MPa	14
4.2	Load Proportionality Factor versus Displacement, Elastic Material, $a=30\text{mm}$, $b=15\text{mm}$, $H=3\text{mm}$, $t=1\text{mm}$, Load Applied: 11 MPa	15
4.3	Load Proportionality Factor versus Displacement, Elastic Perfectly Plastic Material, $a=30\text{mm}$, $b=15\text{mm}$, $H=3\text{mm}$, $t=0.3\text{mm}$, Load Applied: 0.33380 MPa	16
4.4	Load Proportionality Factor versus Displacement, Elastic Perfectly Plastic Material, $a=30\text{mm}$, $b=15\text{mm}$, $H=3\text{mm}$, $t=1\text{mm}$, Load Applied: 11 MPa . .	16
4.5	Load Proportionality Factor versus Displacement, Elastic Perfectly Plastic Material, $a=30\text{mm}$, $b=15\text{mm}$, $H=3\text{mm}$, $t=0.3\text{mm}$, Load Applied: 1 MPa . .	17

4.6	Random Imperfections, $\sigma_f = 0.15t$, a=30mm, b=15mm, H=3mm, t=0.3mm, Load Applied: 0.33380 MPa	17
4.7	Random Imperfections, $\sigma_f = 0.25t$, a=30mm, b=15mm, H=3mm, t=0.3mm, Load Applied: 0.33380 MPa	18
4.8	Random Imperfections, $\sigma_f = 0.15t$, a=30mm, b=15mm, H=3mm, t=0.1mm, Load Applied: 1 MPa	18
4.9	Random Imperfections, $\sigma_f = 0.25t$, a=30mm, b=15mm, H=3mm, t=0.1mm, Load Applied: 1 MPa	19

List of Tables

4.1	Table comparing the critical buckling pressure for different material properties	13
4.2	Table comparing the critical buckling pressure in MPa for different values of COV for elastic perfectly plastic material with random thickness imperfections	15

Nomenclature

- a Dished shell base circle radius/conical shell base radius
- b Radius of top circular flat region
- H Height of the dished shell
- t Thickness of the shell
- E Young's Modulus
- μ Poisson's ratio

Chapter 1

Introduction

Thin shell structures, defined by a high in-plane dimension-to-thickness ratio ($20 \leq a/t \leq 1000$), are extensively used in aerospace, marine, and structural applications due to their excellent load-bearing efficiency and lightweight characteristics. Despite these advantages, their slenderness makes them inherently susceptible to instability and sudden buckling failure, especially under compressive or external pressure loading. In many real-world scenarios, such as pressure vessels or control actuators, shells undergo repeated pressure cycles or fluctuating loads that can trigger instability if the structural response is not well understood or properly designed for.

The presence of small geometric imperfections—arising naturally during manufacturing or assembly—can significantly reduce the buckling strength of thin shells. As a result, modern research emphasizes not only the classical theoretical predictions but also more advanced nonlinear and imperfection-sensitive analyses to better capture real-world behavior (Tripathi et al., 2020; Tripathi et al., 2016).

1.1 Dished Shallow Shells

Among various shell configurations, dished shallow shells present a unique structural form comprising a conical frustum joined at the top with a circular flat or slightly curved plate. This geometry is commonly seen in shallow pressure diaphragms and actuator components (figure 1.1). The distinguishing feature of such shells is the discontinuity in slope at the junction between the frustum and the cap, which leads to complex stress states and deformation modes not observed in pure conical or spherical shells (Tripathi et al., 2016).

Due to these geometric complexities, classical solutions for conical or spherical shells are insufficient to accurately predict the behavior of dished shallow shells. This necessitates a more nuanced analysis that considers both local and global buckling effects, as well as

geometric sensitivity. Prior studies have demonstrated that factors such as frustum angle, cap radius, and thickness play a significant role in influencing the shell's critical buckling pressure and mode shapes (Tripathi et al., 2016).

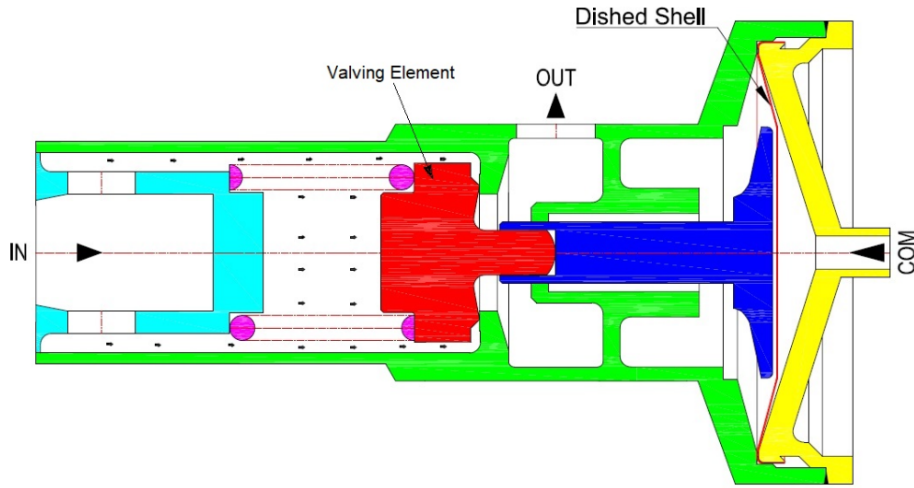


Figure 1.1: Schematic of a control component in which a dished shell is used as an actuator element (Thesis, Surya Mani Tripathi, 2022)

1.2 Snap-Through Buckling

Dished shallow shells under uniform external pressure often exhibit snap-through buckling (figure 1.2), a highly nonlinear instability characterized by a sudden transition from one equilibrium configuration to another. Initially, the shell deforms gradually with increasing pressure until it reaches a critical limit point. Beyond this point, the structure loses stiffness abruptly and ‘snaps’ into a new deformed shape, typically involving large out-of-plane displacements (Tripathi et al., 2020).

This phenomenon is particularly critical for shell components used as mechanical switches or pressure actuators, where the post-buckling configuration is exploited for functionality. To accurately capture this behavior, linear eigenvalue analysis alone is insufficient, as it tends to overestimate the shell's buckling strength. Nonlinear methods such as the Riks analysis are required to trace the full load-deflection path through the limit point and into the post-buckling regime (Majumder et al., 2024).

Additionally, it has been shown that the presence of even small geometric imperfections—either localized dimples or distributed irregularities modeled as random fields—can

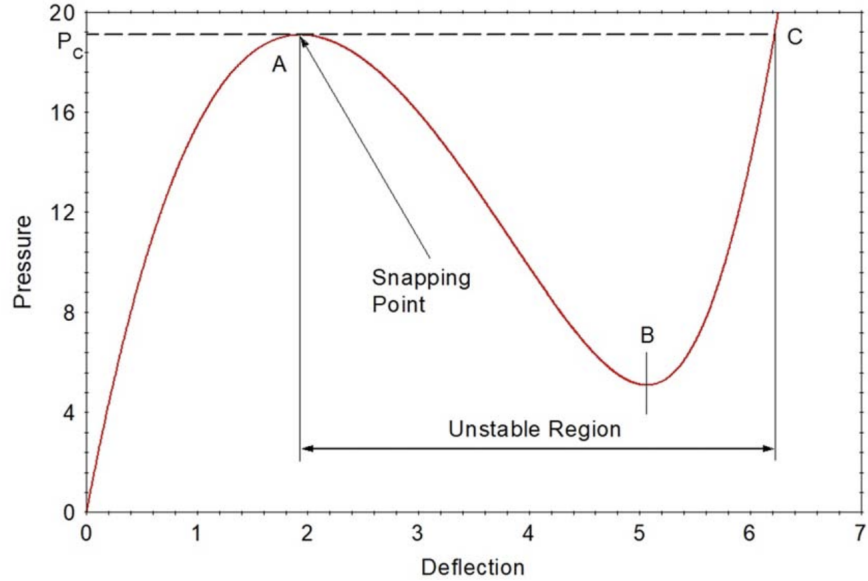


Figure 1.2: Snap-through or Limit Point buckling of a spherical cap under uniform external pressure (S.M. Tripathi, D. Swain, R. Muthukumar, and S. Anup, 2020)

significantly lower the shell's buckling resistance. Therefore, probabilistic and stochastic approaches have become increasingly important in reliability-based shell design (Majumder et al., 2024).

1.3 Random Geometric Imperfections

- Geometric imperfections are introduced in thickness (t) as deviations from the perfect shell geometry (mean geometry) as:

$$t(x, y) = t_0 + f(x, y)t_0 \quad (1.1)$$

where t_0 is the perfect shell thickness and $f(x, y)$ represents random field for t .

- The imperfection magnitudes are given by their r.m.s values.
- The correlations in the random fields are described by the following PSDF (Power Spectral Density Function):

$$S_{ff}(K_x, K_y) = (\sigma_f^2 / 4\pi) b_x b_y \exp[-(1/4)(b_x^2 K_x^2 + b_y^2 K_y^2)] \quad (1.2)$$

where σ_f denotes the r.m.s. of the field;

b_x and b_y denote the characteristic correlation distances and

K_x and K_y denote the wave numbers along $x(\phi)$ and $y(\theta)$, respectively.

- The PSDF model as described above is employed for the simulation of the imperfections using the spectral representation technique.
- The samples for a two-dimensional, stationary, homogeneous, Gaussian field of zero mean are generated as:

$$f(x, y) = \sqrt{2} \sum_{i=1}^{n_x} \sum_{j=1}^{n_y} \sqrt{2S_{ff}(K_x, K_y)\Delta K_x \Delta K_y} \cos(K_x x + K_y y + \phi_{ij}) \quad (1.3)$$

- K_x, K_y represent the discrete wave numbers as:

$$K_x = (i - 1)\Delta K_x \quad K_y = (j - 1)\Delta K_y \quad (1.4)$$

- ϕ_{ij} represents uniformly distributed random phase angles in the range $[0, 2\pi]$
- Beyond cut-off wave numbers (K_x, K_y) , the PSDF ordinates become negligible.
- The increments in the wave numbers ($\Delta K_x, \Delta K_y$) are adopted to be significantly small.
- The FE mesh is made to merge with that of the adopted grid size for the simulation of a random field.

1.4 Objective

The objective of this study is to investigate the buckling behavior of dished shallow shells subjected to uniform external pressure, with a particular focus on the role of geometric imperfections. Thin shell structures are highly sensitive to even minor deviations from their ideal geometry, which often arise during fabrication. These imperfections can significantly affect the critical buckling load and post-buckling response. While classical shell theories provide a first estimate of buckling strength, they often fail to capture the degradation caused by such imperfections. Therefore, this work aims to develop a finite element framework capable of capturing both the ideal and imperfect responses of dished shells. The

goal is to simulate localized imperfections as well as distributed random fields, quantify their influence on critical buckling pressure, and contribute toward a probabilistic design framework for shell structures (Tripathi et al., 2016; Tripathi et al., 2020; Majumder et al., 2024).

1.5 Approach

The dished shallow shell is modeled as a conical frustum closed by a circular plate, representing a common actuator or diaphragm configuration. The geometry is defined with precise dimensional parameters and assigned isotropic linear elastic material properties, with additional simulations including elastic–perfectly plastic behavior to account for yielding. The model is meshed using shell elements (S4R) in Abaqus, and fixed boundary conditions are applied at the base to replicate practical constraints.

The first step in the analysis involves performing a linear eigenvalue buckling study to identify the critical buckling pressure and corresponding mode shapes for the perfect shell. However, since linear analysis does not capture post-buckling behavior or the effects of imperfections, a nonlinear static analysis using the Riks method is then carried out. This allows the full load-deflection path to be traced, including the snap-through instability characteristic of shallow shells under pressure (Tripathi et al., 2020).

To incorporate imperfections, two strategies are followed. First, a dimple-shaped geometric imperfection is introduced by applying a small localized displacement field, and the resulting deformed shape is imported as an initial imperfection. Second, manufacturing-type random imperfections are modeled by introducing spatially varying thickness fields based on a zero-mean Gaussian random field. This is implemented using the spectral representation technique, defined through a prescribed power spectral density function and correlation lengths, as proposed in previous stochastic shell studies (Majumder et al., 2024).

The critical buckling pressures from the perfect and imperfect models are extracted using the maximum load proportionality factor from Riks analysis. These values are used to compute knockdown factors, which quantify the reduction in load-carrying capacity due to imperfections. This structured simulation workflow enables a comparative study of imperfection sensitivity and sets the foundation for a more reliability-focused approach to thin shell design.

Chapter 2

Effect of Linear and Non-Linear Analysis and Dimple Imperfections

2.1 Methodology

This study involves performing linear eigenvalue analysis and non linear riks analysis on dished shallow shells to obtain critical buckling pressure using ABAQUS FE model. The methodology used to perform this analysis are discussed in this chapter.

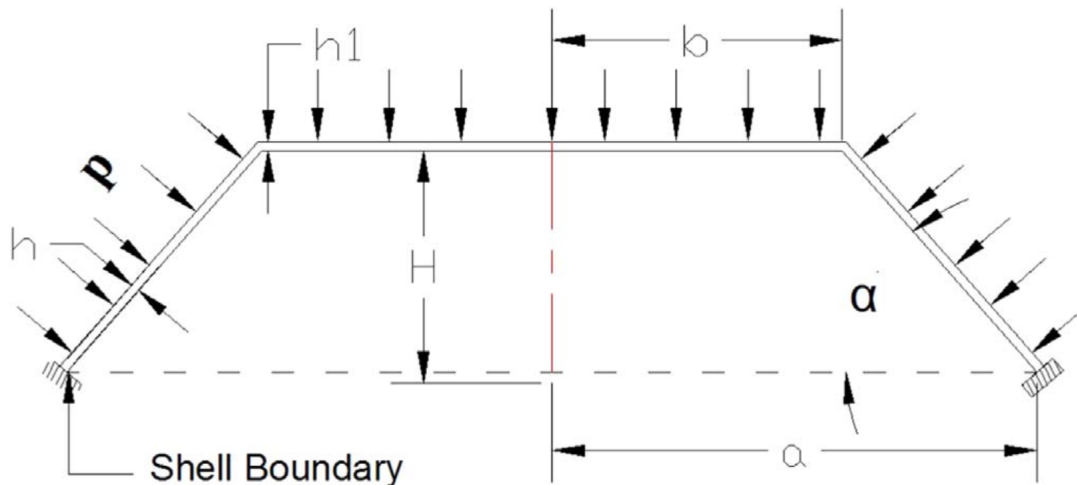


Figure 2.1: A typical dished shell under uniform pressure adopted from Liu et. al. Dong and Shanlin (1997)

The figure 2.1 illustrates the geometry of a representative dished shell examined in this study. Uniformly distributed external pressure, 'P' is applied on the top surface of the shell. The 'H' denotes the height of the shell, 't' denotes the thickness of the shell, 'a' denotes

the base circle radius of the shell and ‘b’ denotes the radius of the top circular region of shell. The bottom edge of the shell is fixed. For this study, the shell is assumed to be of uniform thickness. The effect of material properties and imperfections given in the form of a dimple imperfection on the critical buckling pressure is studied. The FE model used for these cases is explained below.

2.2 Model Description

The current problem was approached on the basis of the following assumptions for analysis:

- The shell is made of uniform thickness.
- The shell material is isotropic and homogeneous.

The FE model in ABAQUS is described as follows:

- A shell geometry was constructed using $a = 30$ mm, $b = 15$ mm, $H = 3$ mm and $t = 0.3$ mm and revolved around a central axis to produce a 3D deformable part.
- The material used is stainless steel ’AISI 321’ (AISI321 (2018)). The material properties are as follows: Elasticity modulus, $E = 200$ GPa, Poisson’s ratio, $\mu = 0.3$ and 0.2% yield strength of 196 MPa.

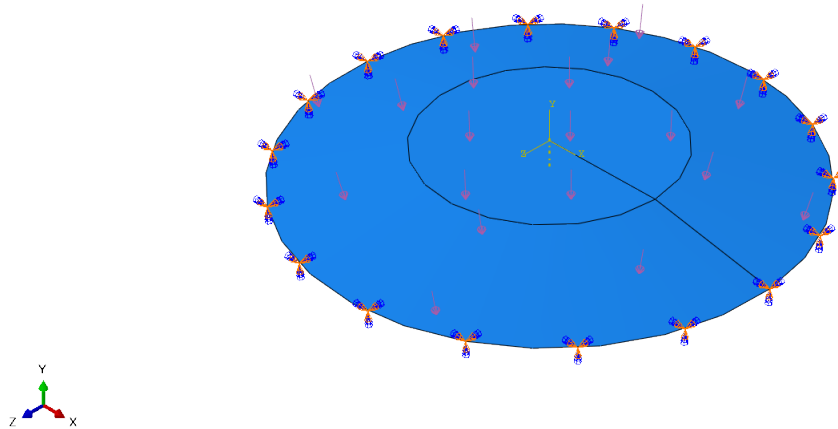


Figure 2.2: Boundary conditions: Pressure load and Fixed bottom edge

- Fixed boundary condition was imposed on the bottom circular edge (figure 2.2), while a uniform pressure of 1 MPa was applied to the top surface, encompassing both the circular and conical regions.

- S4R5' type element is employed for the analysis. The S4R5 element in ABAQUS is a specialized type of finite element used for modeling thin shell structures. This element is a four node, three dimensional element with glass control and reduced integration with five degree of freedom per node (figure 2.3).
- An element size of '0.25 mm' is chosen for all FE analysis being discussed in this article.
- The perturbation buckling method in ABAQUS is used for the linear eigenvalue analysis and a step for this was created to get the eigenmodes and eigen values.
- The General Riks method in ABAQUS is used for the non-linear analysis and a step for the same was created.



Figure 2.3: Quad mesh with element size of 0.25mm - Total of 62929 elements

2.3 Eigenvalue Analysis and Riks Analysis

Eigenvalue Buckling Analysis was conducted to find critical buckling load and mode shapes (figure 2.4) but in linear analysis the strength is overestimated. To get the actual buckling behavior, non linear riks analysis was carried out. The first mode shape was used to understand expected behavior and the first eigenvalue was used as the loading in riks analysis. Riks method enabled nonlinear static analysis, capturing snap-through and post-buckling behavior.

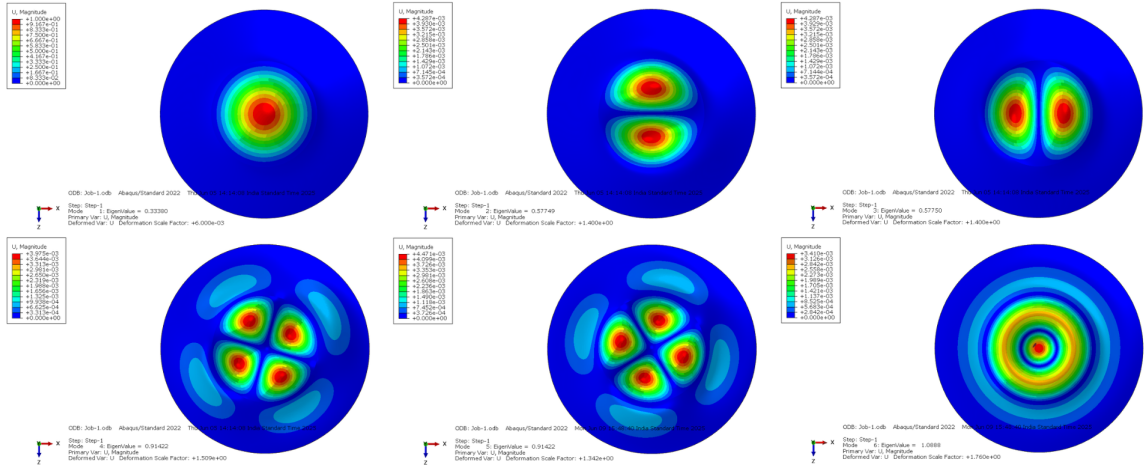


Figure 2.4: Buckling mode shapes for shell of dimensions $a=30\text{mm}$, $b=15\text{mm}$, $H=3\text{mm}$, $t=0.3\text{mm}$

The maximum Load Proportionality Factor (LPF) from Riks analysis gives the Knock-down Factor (KDF), showing how much buckling strength is reduced due to imperfections.

Two shell thicknesses (0.3 mm and 1 mm) were used to carry out riks analysis for perfectly elastic material and elastic-perfectly-plastic material and the critical buckling pressure for them is studied.

The non-linear riks analysis gives a large difference between the critical buckling pressure of perfectly elastic material and elastic-perfectly-plastic material.

2.4 Dimple Imperfections

There can be manufacturing defects in the shell resulting in dimple like imperfections. To cater to those defects we studied the effect of dimple imperfections on the critical buckling pressure.

The dimple imperfection is introduced to the shell by a displacement boundary condition at a very small circular region on the shell. The idea of introducing dimple imperfection in this way if taken from the work of Tejasri Venkat's project report (2024).

The dimples are introduced to the dished shell and the results from the static analysis were introduced as imperfections to the model to carry out nonlinear analysis with elastic-perfectly-plastic material. The dished shell (figure 2.5) with uniform external pressure (1MPa) applied on the top of the shell while the bottom edge is fixed. The orange arrow indicates the displacement boundary condition given for the model. A displacement of 0.03 mm along +Yaxis is given at a circular region of diameter of 0.05 mm. The position of the

dimple is at 5 mm from the central axis of the shell which has the following dimensions: $a = 30$ mm, $b = 15$ mm, $H = 3$ mm, $t = 0.3$ mm.

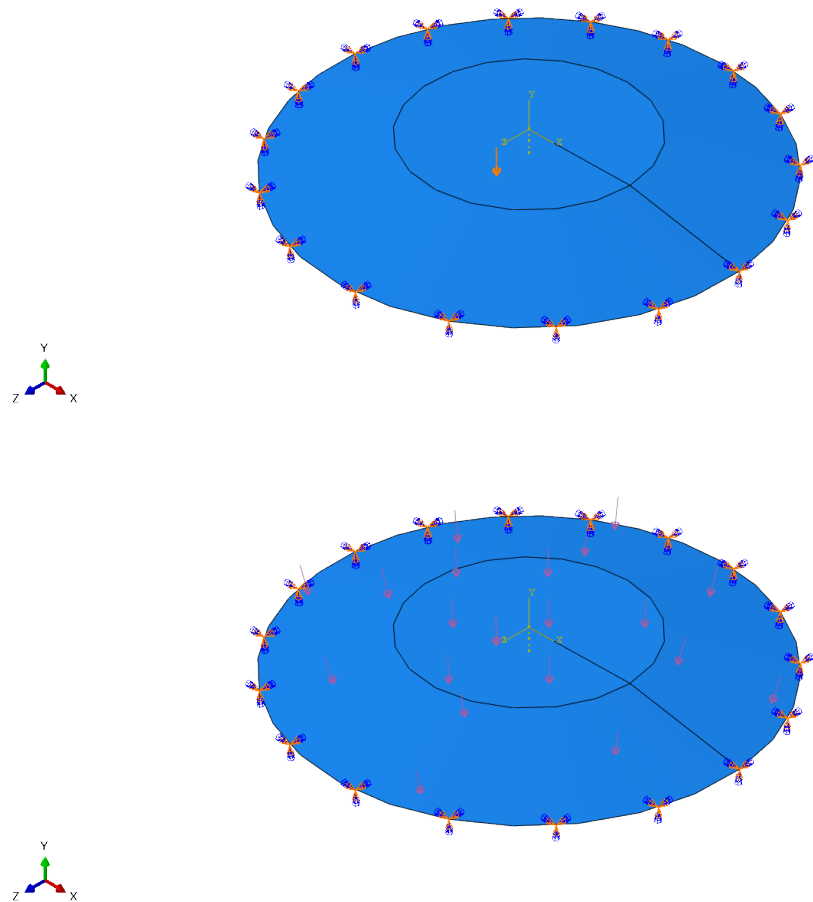


Figure 2.5: Boundary conditions used for static (left) and riks (right) analyses.

Chapter 3

Random Geometric Imperfections

3.1 Background

A significant discrepancy was observed between the theoretical and experimental results. This led to the inclusion of imperfections in the numerical model. We compared the KDFs of perfect shells with those containing dimple and random imperfections. Random imperfections need to be introduced to simulate manufacturing-induced irregularities. Inspired by the work of Majumder et al. (2020) on spherical shells with stochastic imperfections, we adopt a similar approach for dished shallow shells.

3.2 Methodology

To investigate the influence of manufacturing-induced geometric imperfections on the buckling behavior of dished shallow shells, a stochastic thickness variation was introduced into the numerical model. A geometrically perfect dished shallow shell was first modeled in Abaqus, and the nodal coordinates of this baseline mesh were extracted. These coordinates served as the spatial reference for mapping thickness variations defined by a random field.

A Python script was developed to assign node-wise thickness values using a statistically defined random field. The script begins by reading the nodal coordinates and projecting them onto a structured computational grid. Each node is assigned a unique thickness based on a spatially varying Gaussian field, scaled by the desired mean and standard deviation. The output is a ‘.csv’ file containing the node numbers and their corresponding thickness values. This file is used to introduce the thickness field into Abaqus through Discrete Fields, enabling spatially varying shell thicknesses during simulation.

The random field itself was generated within the script using the spectral representation

method, a widely accepted approach for simulating homogeneous, stationary Gaussian random fields. The field was constructed as a superposition of cosine functions, with random phase shifts and amplitudes weighted by a prescribed Power Spectral Density Function (PSDF). This formulation ensures a statistically consistent spatial correlation structure governed by the chosen characteristic correlation lengths and wave numbers. The root mean square (r.m.s.) value of the field was adjusted to achieve the desired magnitude of imperfections. To visualize the random field and verify its qualitative structure, a MATLAB routine was used to plot $f(x, y)$ on a 100x100 grid; a new field is generated with each run, offering a visual representation of the randomness (Figure 3.1). Care was taken to ensure that the grid resolution of the generated field aligned with the finite element mesh, ensuring accurate mapping of thickness values across the model.

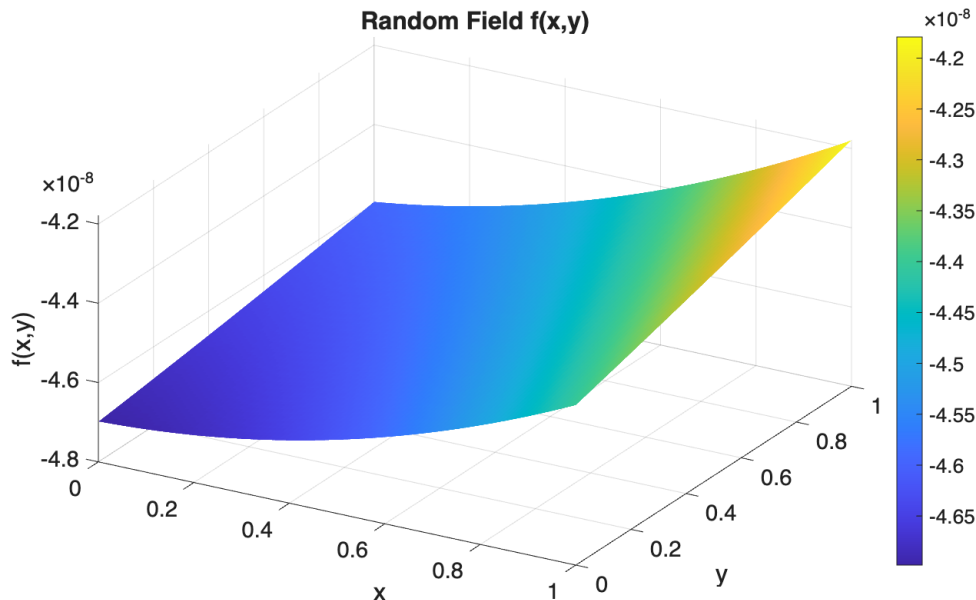


Figure 3.1: Sample Random field for thickness variation

The procedure was applied to two shell models with nominal thicknesses of 0.3 mm and 1 mm. For each model, random fields with 15% and 25% coefficient of variation (COV) were generated to represent varying degrees of imperfection severity. Each execution of the script results in a new realization of the random field, allowing multiple statistically independent simulations to be carried out as part of a stochastic study. This framework provides insight into the sensitivity of the post-buckling behavior to spatial imperfections in shell thickness.

Chapter 4

Results and Discussion

This chapter covers the results and discussion of the data obtained from the analysis done as explained in chapter 2 and 3. The effect of dimple imperfections on the critical buckling pressure for perfectly elastic material and elastic-perfectly plastic material is studied. The effect of random geometric imperfections are studied in chapter 3. The results are discussed in the same order.

4.1 Eigenvalue and Riks Analysis

The critical buckling pressure when the eigenvalue analysis is carried out comes out to be 0.33380 MPa. The critical buckling pressure for riks analysis with perfectly elastic material properties and thickness 0.3 mm (figure 4.1) comes out to be = 0.74964804 MPa. The critical buckling pressure for riks analysis with perfectly elastic material properties and thickness 1 mm (figure 4.2) comes out to be = 7.77701951 MPa. The critical buckling pressure for riks analysis with elastic perfectly plastic material properties and thickness 0.3 mm (figure 4.3) comes out to be = 0.259498 MPa. The critical buckling pressure for riks analysis with elastic perfectly plastic material properties and thickness 1 mm (figure 4.4) comes out to be = 1.652598935 MPa.

Table 4.1: Table comparing the critical buckling pressure for different material properties

Thickness	0.3 mm	1 mm
Elastic LPF (MPa)	0.74964804	7.77701951
Elastic-perfectly-plastic LPF (MPa)	0.259498	1.652598935

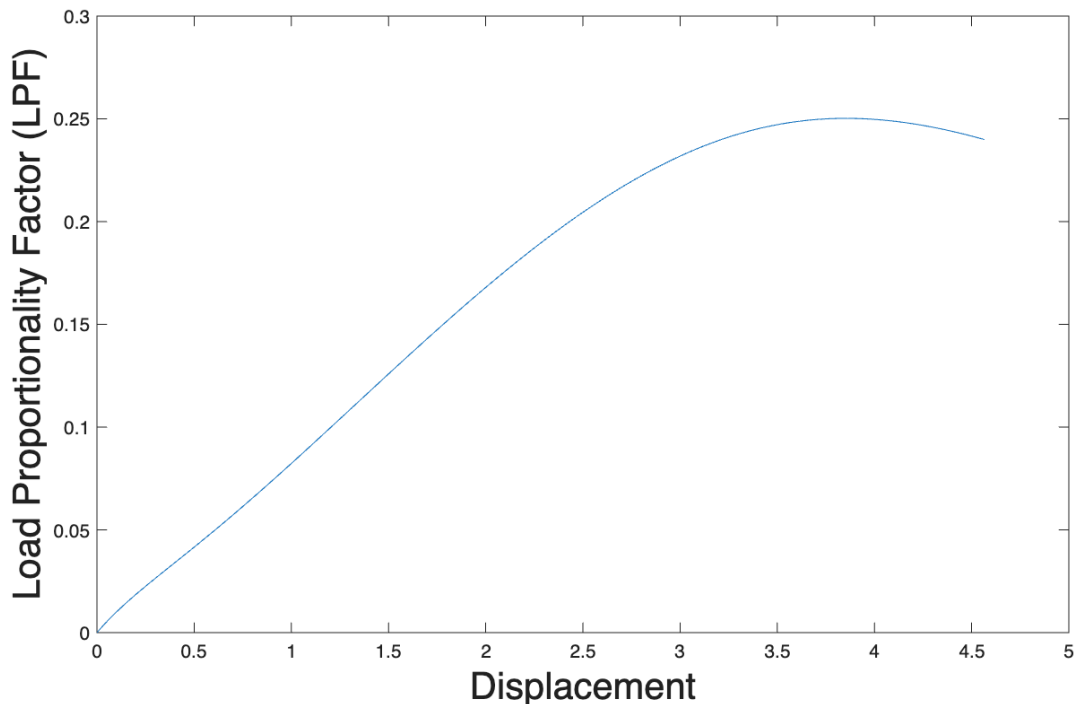


Figure 4.1: Load Proportionality Factor versus Displacement, Elastic Material, $a=30\text{mm}$, $b=15\text{mm}$, $H=3\text{mm}$, $t=0.3\text{mm}$, Load Applied: 0.33380 MPa

4.2 Dimple Imperfections

The critical buckling pressure for a dimple imperfection (figure 4.5) with elastic-perfectly-plastic material properties comes out to be = 0.258614 MPa.

4.3 Random Imperfections

The critical buckling pressure for random imperfections in the shell thickness for 0.3 mm mean thickness and 15% COV (figure 4.6) come out to be 0.259498457 MPa. For 0.3 mm mean thickness and 25% COV (figure 4.7) the critical buckling pressure comes out to be 0.259498123 MPa. For 0.1 mm mean thickness and 15% COV (figure 4.8) it is 0.0460634 MPa and for 0.1 mm mean thickness, 25% COV (figure 4.9) it is 0.0460628 MPa.

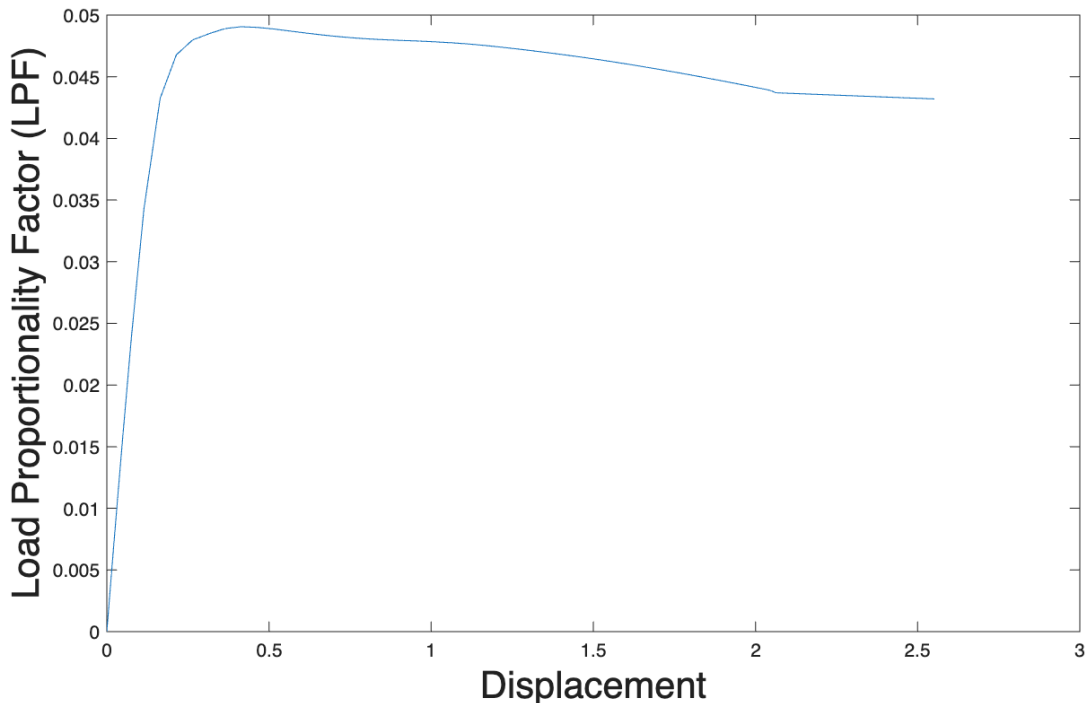


Figure 4.2: Load Proportionality Factor versus Displacement, Elastic Material, $a=30\text{mm}$, $b=15\text{mm}$, $H=3\text{mm}$, $t=1\text{mm}$, Load Applied: 11 MPa

Table 4.2: Table comparing the critical buckling pressure in MPa for different values of COV for elastic perfectly plastic material with random thickness imperfections

Thickness	0.3 mm	0.1 mm
Critical Pressure for 15% COV	0.259498457	0.0460634
Critical Pressure for 25% COV	0.259498123	0.0460628

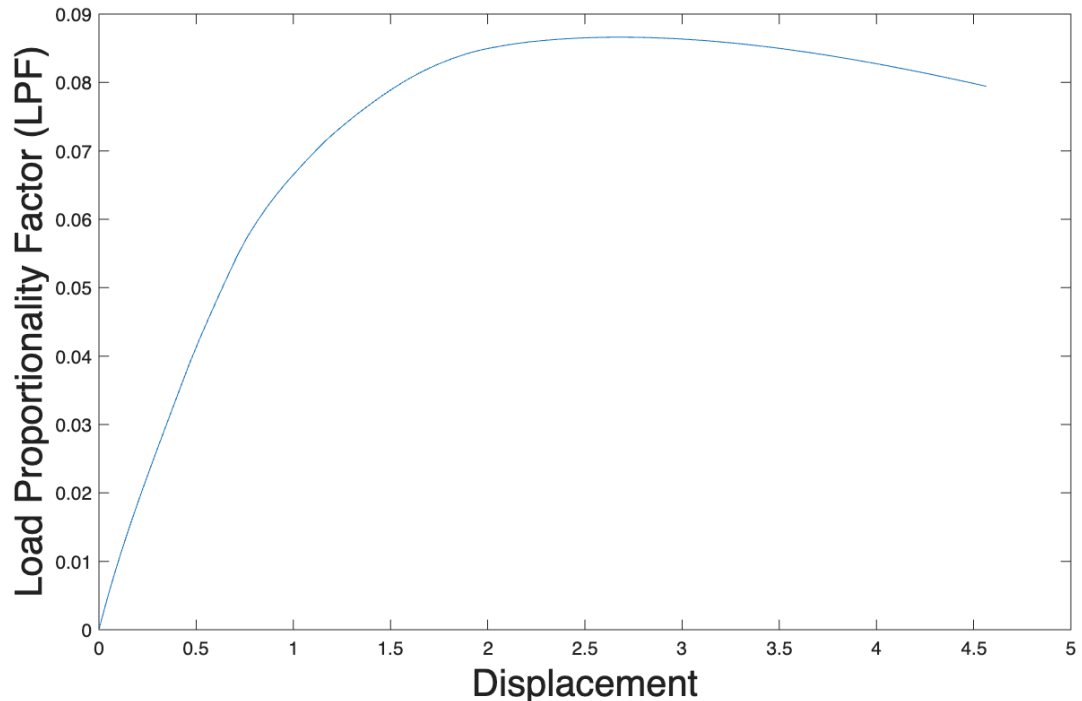


Figure 4.3: Load Proportionality Factor versus Displacement, Elastic Perfectly Plastic Material, $a=30\text{mm}$, $b=15\text{mm}$, $H=3\text{mm}$, $t=0.3\text{mm}$, Load Applied: 0.33380 MPa

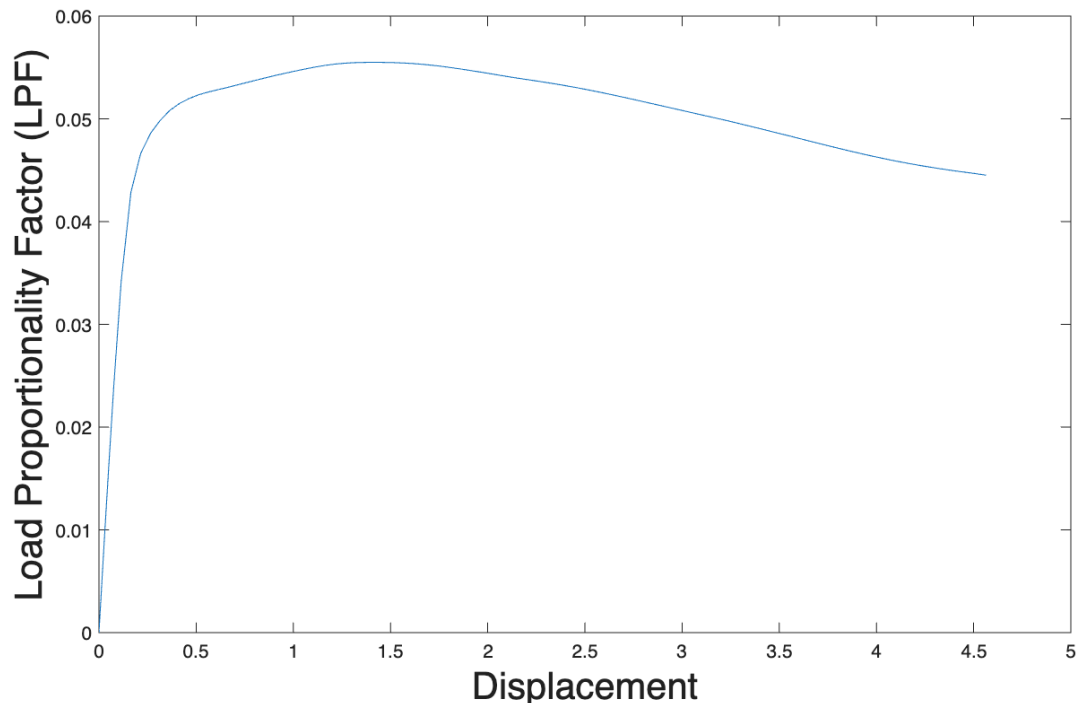


Figure 4.4: Load Proportionality Factor versus Displacement, Elastic Perfectly Plastic Material, $a=30\text{mm}$, $b=15\text{mm}$, $H=3\text{mm}$, $t=1\text{mm}$, Load Applied: 11 MPa

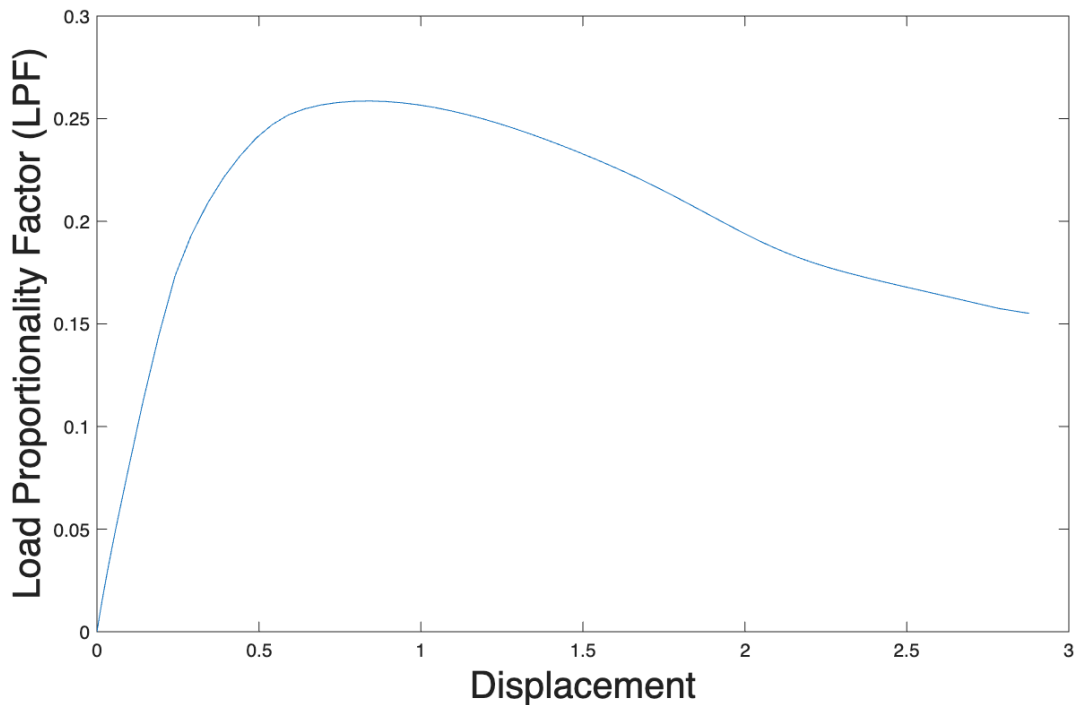


Figure 4.5: Load Proportionality Factor versus Displacement, Elastic Perfectly Plastic Material, $a=30\text{mm}$, $b=15\text{mm}$, $H=3\text{mm}$, $t=0.3\text{mm}$, Load Applied: 1 MPa

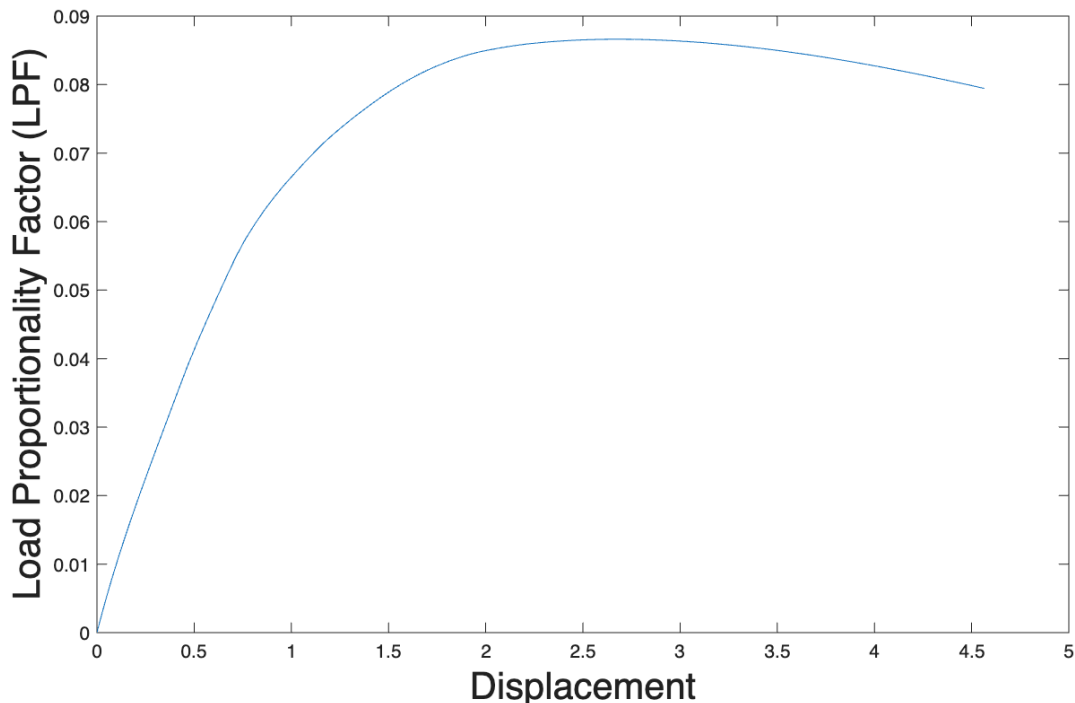


Figure 4.6: Random Imperfections, $\sigma_f = 0.15t$, $a=30\text{mm}$, $b=15\text{mm}$, $H=3\text{mm}$, $t=0.3\text{mm}$, Load Applied: 0.33380 MPa

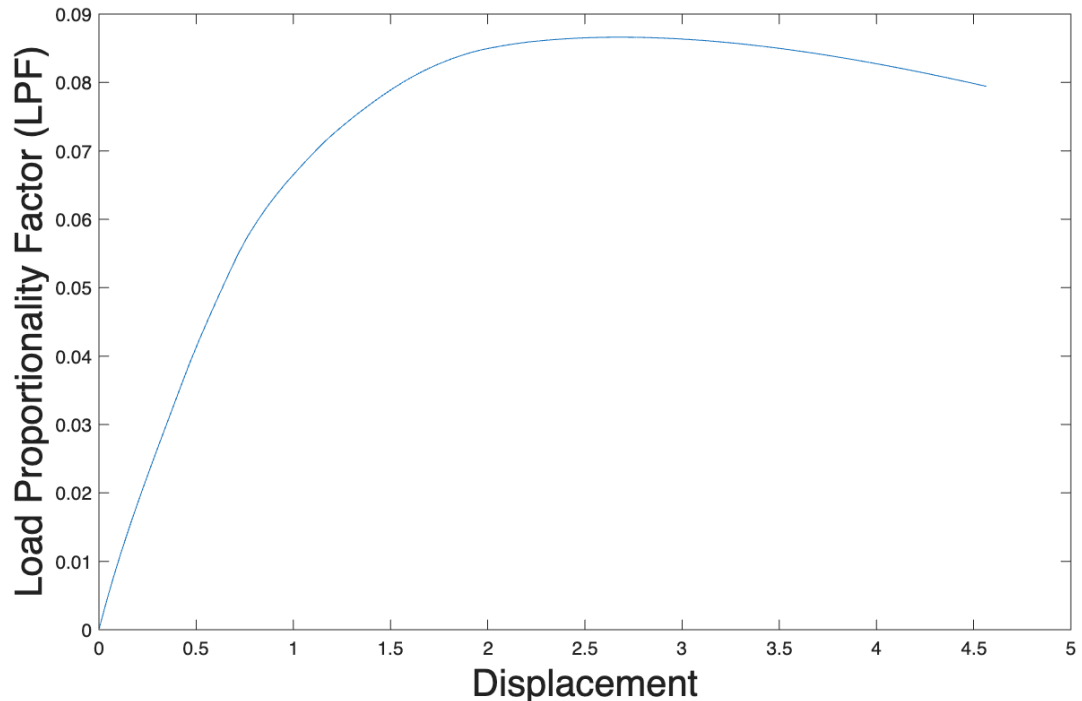


Figure 4.7: Random Imperfections, $\sigma_f = 0.25t$, $a=30\text{mm}$, $b=15\text{mm}$, $H=3\text{mm}$, $t=0.3\text{mm}$, Load Applied: 0.33380 MPa

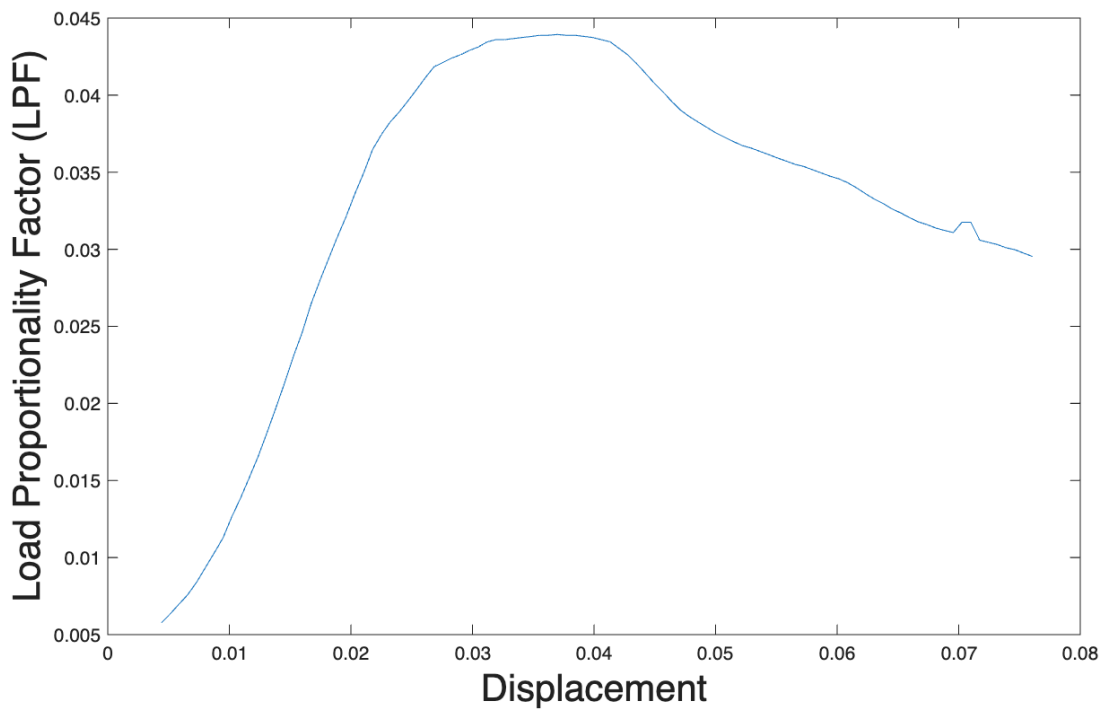


Figure 4.8: Random Imperfections, $\sigma_f = 0.15t$, $a=30\text{mm}$, $b=15\text{mm}$, $H=3\text{mm}$, $t=0.1\text{mm}$, Load Applied: 1 MPa

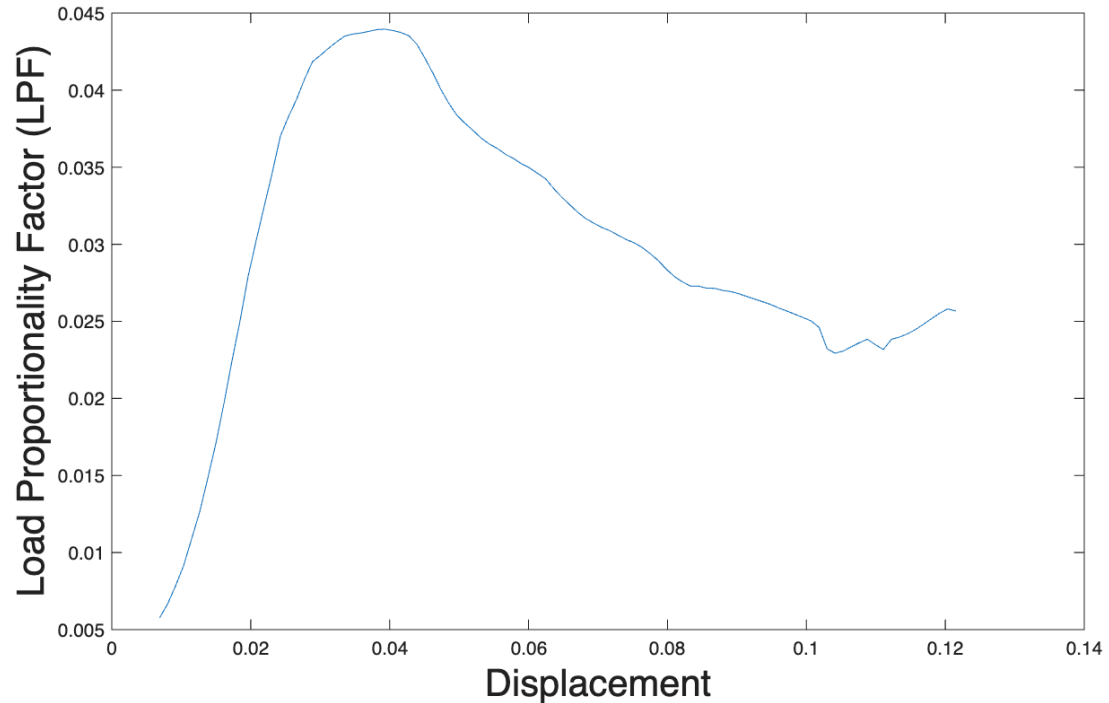


Figure 4.9: Random Imperfections, $\sigma_f = 0.25t$, $a=30\text{mm}$, $b=15\text{mm}$, $H=3\text{mm}$, $t=0.1\text{mm}$, Load Applied: 1 MPa

Chapter 5

Conclusion

This study investigated the buckling behavior of dished shallow shells under uniform external pressure, emphasizing the impact of both material nonlinearities and geometric imperfections. Using a finite-element framework in Abaqus, we compared ideal shells and imperfect configurations via linear eigenvalue and nonlinear Riks methods. The linear buckling analysis was shown to significantly overestimate the collapse pressure, whereas the Riks method accurately captures snap-through instability and the full post-buckling response.

From the Riks results summarized in Table 4.1, the elastic LPF for a 0.3 mm shell of 0.7496 MPa falls by over 65% to 0.2595 MPa when plasticity is included. For the 1 mm shell, LPF diminishes by nearly 79% (from 7.7770 MPa to 1.6526 MPa), underscoring that accounting for yielding is critical for realistic strength predictions. Introducing geometric imperfections yields only marginal additional knockdowns: localized dimples and spatially correlated thickness variations (up to 25% COV) each alter the LPF by less than 1% (Table 4.1 vs. Table 4.2). Even at a thinner mean of 0.1 mm, increasing COV from 15% (0.0460634 MPa) to 25% (0.0460628 MPa) produces a virtually negligible change, indicating that once plastic collapse dominates, further thickness variability has minimal effect.

Overall, these tables demonstrate that (1) material nonlinearity is the principal driver of strength reduction—demanding Riks-based collapse analyses—and (2) moderate geometric imperfections, whether dimples or random fields, impart only incremental knockdowns in the regimes studied. This work establishes a comprehensive simulation-based approach to assess thin-shell reliability and lays a foundation for probabilistic design methodologies that explicitly account for manufacturing uncertainties.

Building on this framework, future studies should explore alternative loading conditions and material nonlinearities, but most critically expand the imperfection modeling to

include random geometric deviations specifically in the bottom radius of the shell. Implementing such imperfections—and providing the associated generation scripts—will deepen our understanding of buckling sensitivity in the most structurally critical regions and further enhance the reproducibility of the probabilistic design approach.

Chapter 6

References

Surya Mani Tripathi, Anup S, R. (2016), ‘Effect of geometrical parameters on mode shape and critical buckling load of dished shells under external pressure’, *Thin Walled Structures* 106, 218–227.

Surya Mani Tripathi, Digendranath Swain, R. M. S. A. (2020), ‘Investigation on snap-through buckling behavior of dished shells under uniform external pressure’, *Journal of Applied Mechanics* 87(12), 121001.

Vissarion Papadopoulos, Manolis Papadrakakis (2004), ‘Finite-Element Analysis of Cylindrical Panels with Random Initial Imperfections’, *Journal of Engineering Mechanics* 130(8), 867–876.

Rohan Majumder, Sudib K. Mishra, Subrata Chakraborty (2024), ‘A Reliability-based design against post-buckling load drop in spherical shell cap with stochastic imperfections’, *International Journal of Non-Linear Mechanics* 165, 104794.

Appendix A

Methodology for Generating Random Thickness Imperfections

A.1 Overview

To capture manufacturing-induced geometric variability in the shell's thickness, a stochastic Fourier-based random field was superimposed on the nominal shell thickness. This approach produces a spatially correlated thickness imperfection map $t(x, y)$ with a prescribed root-mean-square (rms) amplitude and correlation lengths in the x and y directions.

A.2 Implementation Details

The Python script performs the following steps:

1. Parameter definition

```
1 b_x, b_y      = 0.015, 0.015          # Correlation lengths [m]
2 $del_k_x$, del_k_y$ = 0.0366, 0.0168   # Spectral increments
3 [1/m]
4 rms           = 15e-6                  # Desired rms amplitude [m]
5 t0            = 0.0001                 # Nominal thickness [m]
6 n_x, n_y     = 96, 96                  # Number of spectral modes
```

2. Reading nodal coordinates

A CSV file containing columns ‘NodeLabel’, ‘X’, ‘Y’ is loaded and sorted by node label.

3. Random-phase generation

‘ ϕ_{ij} ’ is sampled uniformly in $[0, 2\pi]$ for each mode.

4. Spectral amplitude computation

The spectral density S_{ff} and mode amplitude A_{ij} are computed per the equations above.

5. Field synthesis

The nested loops over modes accumulate $f(x, y)$ at each nodal location (x, y) . The field is mean-corrected, then added to t_0 .

6. Output

An output CSV mapping each ‘ElementID’ (equal to ‘NodeLabel’) to its perturbed ‘Thickness’.

A.3 Code Availability

All scripts and example data files used for imperfection generation are publicly available at:

GitHub: <https://github.com/divyachoudhary22/IIST-Summer-Internship>

Users can clone the repository, adjust ‘rms’, ‘ b_x ’, ‘ b_y ’, or grid resolution (‘ n_x ’, ‘ n_y ’), and reproduce the exact random-field realizations by setting a fixed NumPy random seed.